catalysts

MDPI

Article

Impact of H_2O_2 on the Lactic and Formic Acid Degradation in Presence of TiO_2 Rutile and Anatase Phases under UV and Visible Light

Annika Holm [1,2], Marwa Hamandi [1], Karima Sahel [3], Frederic Dappozze [1] and Chantal Guillard [1,*]

1 University of Lyon, Université Claude Bernard Lyon 1, 2 avenue Albert Einstein, F-69626 Villeurbanne, France; arholm2@illinois.edu (A.H.); marwahmandi@gmail.com (M.H.); frederic.dappozze@ircelyon.univ-lyon1.fr (F.D.)

2 Chemistry Department, Sonoma State University (SSU), 1801 East Cotative Ave, Rohnert Park, CA 94928, USA

3 Laboratoire des Eco-Matériaux Fonctionnels et Nanostructurés, Faculté de Chimie, Département Génie des Matériaux, Université des Sciences et de la Technologie d'Oran (USTO), Bir El Djir 3100, Algeria; sahel_karima2002@yahoo.fr

* Correspondence: chantal.guillard@ircelyon.univ-lyon1.fr; Tel.: +33-472-445-316

Received: 27 August 2020; Accepted: 21 September 2020; Published: 1 October 2020

Abstract: The degradation rates of formic acid and lactic acid in the presence and absence of H_2O_2 were studied, utilizing several TiO_2 catalysts: PC105 (100% anatase), MPT 625 (100% rutile), and P25 (80% anatase/20% rutile), and the results were discussed with regards to the current literature. The impact of hydrogen peroxide on the photocatalytic efficiency of eleven TiO_2 samples was then determined, using commercial anatase structures (PC105, PC500, UV100), commercial mixed anatase/rutile (P25 and P90), and six rutile (two commercial samples: MPT 625 and C-R160, and four home-made rutile samples were synthesized by $TiCl_4$ hydrolysis). The effect of catalyst surface area and TiO_2 phase on the degradation rate of lactic acid (LA) and the decomposition of H_2O_2 was studied and discussed in regard to the active species generated. The intermediate products formed in the absence and presence of H_2O_2 were also an important factor in the comparison. Finally, the efficiency of the degradation of LA and formic acid (FA) in the presence of rutile and H_2O_2 was determined under visible light, and their reactivity was compared. The intermediate products formed in the degradation of LA were identified and quantified and compared to those obtained under UV (Ultra-Violet).

Keywords: photocatalysis; UV; visible light; TiO_2; rutile; anatase; H_2O_2

1. Introduction

Several publications [1–14] have mentioned the impact that H_2O_2 addition has on the degradation of different organic compounds in the presence of TiO_2. Most studies performed using P25 TiO_2 found that H_2O_2 has a favorable impact. It was explained by the elevated hydroxyl radical production, either due to hydrogen peroxide's reaction with conduction band electrons, or to indirect formation via $O_2^{\circ -}$, which is generated by the reduction of water and is able to avoid electron–hole recombination (Equations (1) and (2)).

$$H_2O_2 + e^- \rightarrow OH^\circ + OH^- \quad (1)$$

$$H_2O_2 + O_2^{-\circ} \rightarrow OH^\circ + OH^- + O_2 \quad (2)$$

However, some researchers have also shown an unfavorable effect of H_2O_2 on TiO_2 [2,3] which is explained by the competition between H_2O_2 and a pollutant for the adsorption sites. H_2O_2 is also proposed to be in competition with photoproduced holes, since H_2O_2 competes with the reaction of water (Equation (3)), which limits the formation of OH radicals (Equations (3) and (4)):

$$H_2O_2 + h^+ \rightarrow H^+ + HO_2^{\circ} \quad (3)$$

$$H_2O + h^+ \rightarrow H^+ + OH^{\circ} \quad (4)$$

To our knowledge, the impact of anatase and rutile phase on the UV degradation of organic molecules in the presence of H_2O_2 has not been well studied, and the interpretation of the results is still under debate [1,15]. H_2O_2 seems to always have a higher impact in the presence of rutile TiO_2 under UV irradiation. While differences in the nature of peroxo-complex formation on the surface of anatase and rutile phases was suggested by Ohno et al. [1], Tang et al. [15] reported that the difference could be attributed to a heterogeneous reaction on the particle surface of the photocatalyst for anatase TiO_2, and a reaction in solution for rutile TiO_2.

Contrary to the latter hypothesis, it is well known that in the presence of H_2O_2 a complex is formed on the surface of TiO_2, allowing for H_2O_2 decomposition. Moreover, several publications report the decomposition of this peroxo-complex on rutile and anatase phase in the absence of pollutants and show that the decomposition of H_2O_2 is favored on rutile phase. These results are in agreement with the work of Hirakawa et al. [16] and Zhang et al. [17]. Both publications provide evidence of an increase in OH° radical formation by the addition of hydrogen peroxide on rutile and rutile-containing TiO_2, and a decrease in $O_2^{-\circ}$ formation. For anatase TiO_2, a decrease in OH° radical formation and an increased formation of $O_2^{-\circ}$ were observed. However, to our knowledge, no connections have been made in previous works on the impact that pollutants have on these results.

Several other works were also published on the possibility of using visible light to degrade pollutants in the presence of TiO_2 and H_2O_2, and have mentioned the activation of the peroxo-complex formed on the surface of TiO_2 [15,18–21]. However, no comparison was made between the impact of H_2O_2 on the efficiency of TiO_2 under UV and visible light.

Many other issues remain subject to debate: is the favorable or unfavorable impact of H_2O_2 dependent on the surface area of the catalyst? Is there a correlation between the disappearance rate of organic compounds and the disappearance rate of H_2O_2? What is the impact of H_2O_2 on the formation of intermediate products? What is the efficiency of H_2O_2/rutile under visible light in comparison to UV? Is the mechanism similar under UV and visible activation?

The objective of our work is to try to answer to some of these questions using two pollutants: formic acid and lactic acid. We also plan to utilize several rutile, anatase and mixed phase photocatalysts with varying surface areas under UV irradiation. Finally, we plan to draw a comparison between the H_2O_2/rutile efficiency under UV and visible light using formic acid and lactic acid.

2. Results and Discussion

2.1. Comparison of the Impact of H_2O_2 on Formic and Lactic Acid Photocatalytic Degradation in Presence of P25, PC105 and C-R100

Before studying the impact of H_2O_2 on formic acid and lactic acid degradation, a control experiment was carried out with H_2O_2 in the dark. No oxidation of formic acid and lactic acid was observed within a 2 h period of darkness at room temperature, indicating that the possible degradation of hydrogen peroxide in the absence of light can be ruled out for all experiments. Similarly, control experiments using UV irradiation in the absence of a photocatalyst (while maintaining constant pollutant and H_2O_2 concentrations) confirm the lack of photolysis.

The impact of H_2O_2 on lactic acid and formic acid was then determined in the presence of three commercial TiO_2 samples: PC105, C-R100 and P25—a commonly used reference in photocatalysis.

The disappearance rate of these two organic compounds was represented as a function of time in the presence and absence of H_2O_2 (Figure 1).

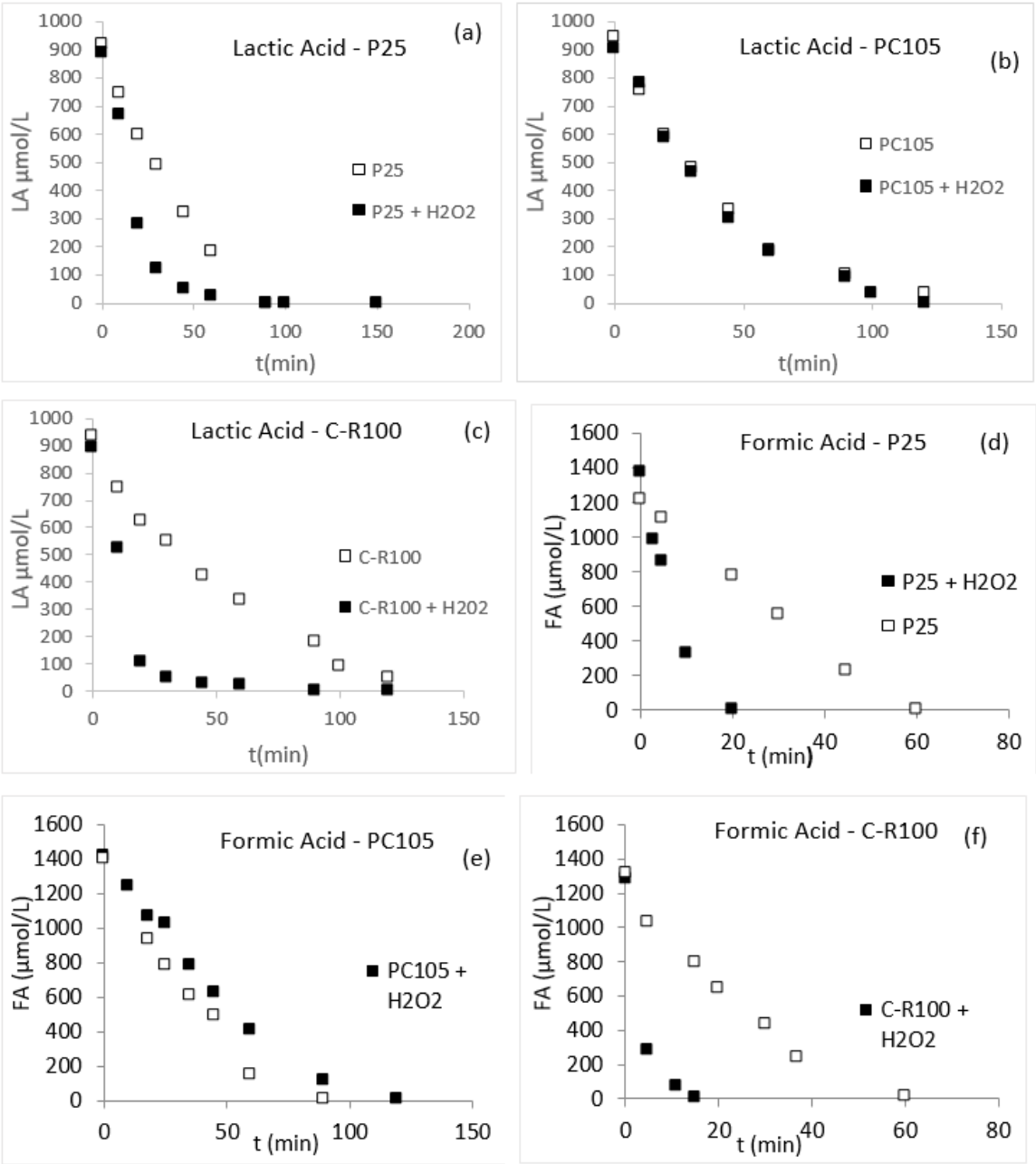

Figure 1. Degradation of lactic acid (**a**–**c**) and formic acid (**d**–**f**) in the presence of P-25, PC105 and C-R100, respectively.

Regardless of which organic compound was used, the same behavior was observed: a significant improvement of the degradation rate in the presence of rutile phase TiO_2 (Figure 1a,c,d,f), and no impact or a slightly negative impact in the presence of pure anatase phase.

Few works have studied the impact of the anatase and rutile phase on the degradation of organic molecules in the presence of H_2O_2, and the interpretation of their results is still subject to debate [1,15]. In all cases, the authors found that H_2O_2 had a greater impact in the presence of rutile TiO_2 and under UV irradiation, which agrees with our results. While Ohno et al. [1] suggested that the difference is due to the nature of the H_2O_2 complex formed, Tang et al. [15] suggested that photodegradation catalyzed

by rutile TiO_2 occurs mainly in the solution, but takes place on the surface of the photocatalyst when anatase TiO_2 is present.

Further explanations have been published using experiments performed in the absence of pollutant [16,17,22], which show a difference in the nature of Reactive Oxygen Species (ROS) generation on the two TiO_2 phases in the presence of H_2O_2. The authors found that when H_2O_2 is utilized, hydroxyl radicals (OH°) are primarily generated on rutile TiO_2, while in the presence of anatase TiO_2, hydroperoxide radical ($HO_2°$) (a much fewer active species) formation predominates [16,17]. These differences are explained by the formation of alternate H_2O_2 complexes on TiO_2: Ti–η^2-peroxide on the surface of rutile, and Ti–μ-peroxide on the surface anatase [17]. Although Density Functional Theory (DFT) analyses indicate that for both phases the more favorable structure of the Ti–peroxo-complex is Ti–O–O–H [23,24].

The differences in the reduction and oxidation properties of these two phases were suggested by our previous results [22] and evaluated by the determination of conduction band energies [25]. It was found that the Conduction Band (CB) edge of rutile TiO_2 is localized at a lower potential than the CB of anatase, inducing a stronger reducing potential for rutile TiO_2. On the surface of rutile TiO_2, a direct reduction of H_2O_2 or indirect reaction between $O_2^{°-}$ and H_2O_2 (Equations (1) and (2)) would likely occur. While on anatase TiO_2, due to its stronger oxidizing potential, H_2O_2 is primarily oxidized into $HO_2^{°-}$ (Equation (3)) in competition with water (Equation (4)).

According to these various studies, the greater impact of H_2O_2 on rutile phase TiO_2 can be explained by a higher production of OH° due to differences in the oxydo-reduction properties of rutile and anatase.

2.2. Impact of H_2O_2 on the Photocatalytic Degradation of Lactic in Presence of Different TiO_2 Rutile, TiO_2 Anatase and Mixture of These Both Phases

The impact of hydrogen peroxide on lactic acid (LA) degradation was determined in the presence of two commercial rutile, three commercial anatase, and two mixed phase TiO_2 samples. Experiments were also conducted using four home-made rutile samples. The LA degradation rates obtained in the presence and absence of H_2O_2 are reported in Figure 2a.

As formerly observed and discussed in the previous paragraph, a substantially positive impact on rutile TiO_2 (C-R160 is an exception) was observed, while no impact or a slightly negative impact was observed for the pure anatase phase, shown in Figure 2b by representing the ratio of the LA degradation rate with and without H_2O_2.

In addition to differences between the rutile and anatase phases, some differences are also observed within the same phase. H_2O_2 had a significantly positive impact on our two home-made TiO_2 rutile samples, which were both calcined after 2 and 48 h of hydrolysis. Improvement factors of 10 and 18 were found, respectively. Moreover, the lactic acid degradation rates on these two catalysts in the presence of H_2O_2 are about 1.4 times higher than that of TiO_2 P25, an international reference in the photocatalytic field.

The lack of a positive impact on LA degradation in the presence of C-R160 and its low efficiency are attributed to the presence of surface impurities observed by the release of organic acid in water, and by the presence of about 5% Si. On the one hand, the presence of SiO_2 on TiO_2 surface modifies the adsorption properties of LA due to the ZPC (zero point charge) of silica which is about 2 and favors the recombination of (e^-, h^+) pairs, on the other hand, the organic impurities present in C-R160 are degraded in competition with LA degradation.

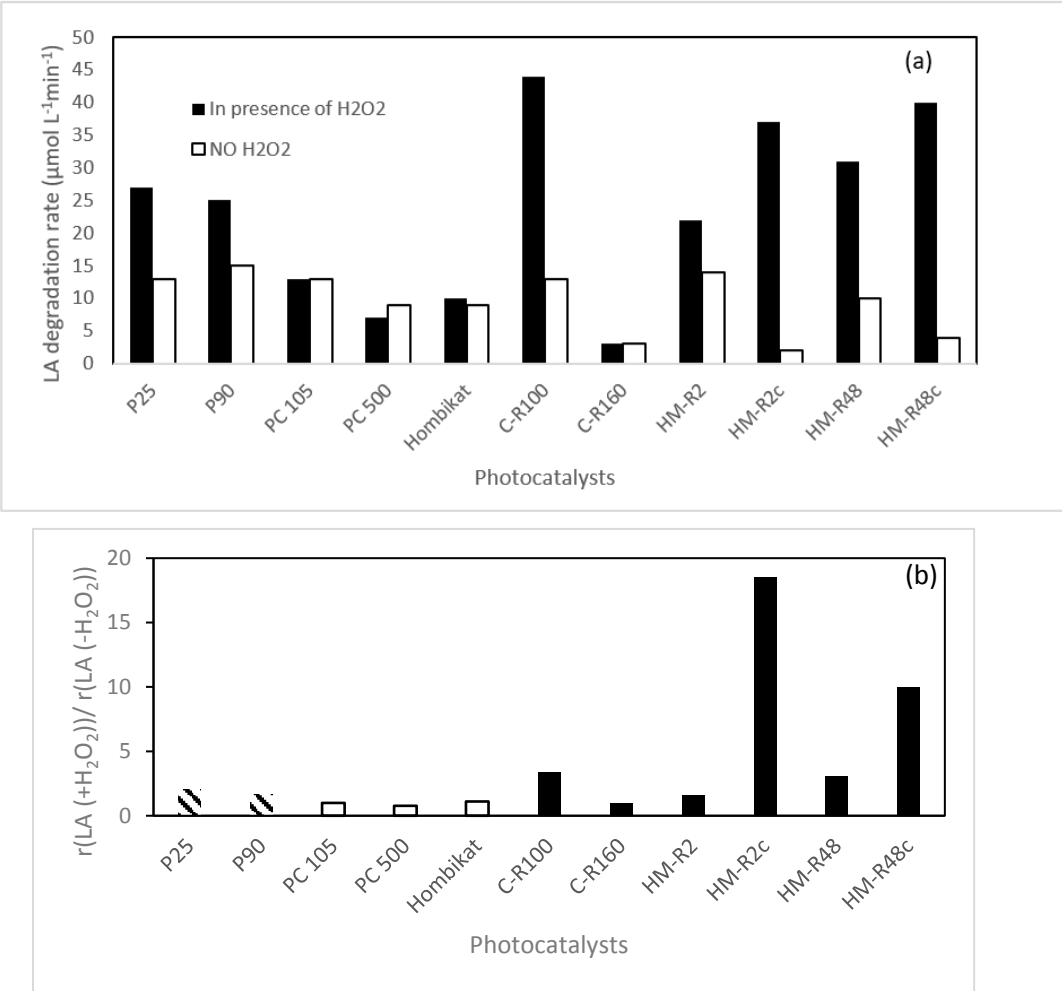

Figure 2. (**a**) Lactic acid degradation rates in the presence of pure rutile, anatase and mixed phase TiO_2, and (**b**) the ratio of lactic acid (LA) degradation rate with and without H_2O_2 in the presence of pure rutile, anatase, and mixed phase TiO_2. The dashed horizontal line corresponds to a ratio of 1 (LA degradation rate equivalent in the presence or absence of H_2O_2).

The slightly improved efficiency of MPT-625 (C-R100) towards lactic acid degradation in the presence of H_2O_2 could be partly attributed to the photo-Fenton reaction caused by the presence of iron in the structure, which was observed by Inductively Coupled Plasma (ICP) and X-ray photoelectron spectrometry (XPS).

Considering our home-made rutile TiO_2 samples, the most efficient catalysts are those which have been calcined at 300 °C. A likely cause is the improvement in crystallinity which favors the formation of OH° radicals. It can also be attributed to a decrease in pore volume. After calcination, the volume of the pores are 2.2 and 1.7 10^{-2} cm^3g^{-1} for HM-R2c and HMr-R48c, respectively, while prior to calcination, the pore volumes were 0.7 and 0.9 10^{-2} cm^3g^{-1} [18].

Moreover, it is apparent that the larger the surface area, the less lactic acid is degraded in the presence of H_2O_2 (Figure 3). Similar behavior was also observed for the pure anatase phase (Figure 3). While the impact is significant on the rutile phase, in the presence of pure anatase or anatase mixed with 20% rutile TiO_2, an increase in the surface area has much less of an impact.

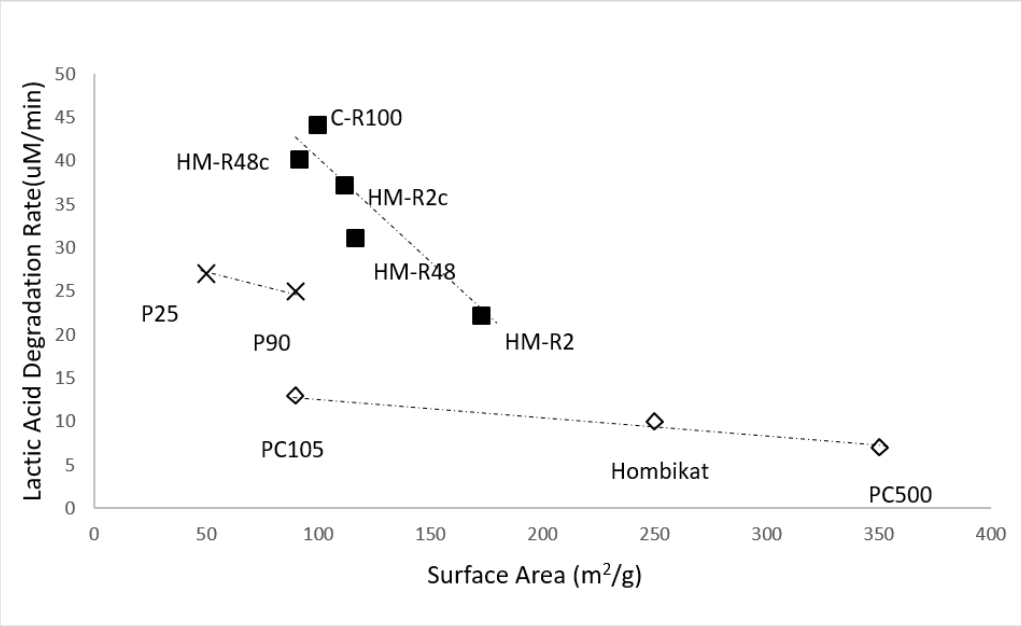

Figure 3. Impact of the surface area on LA degradation in the presence of rutile TiO_2 (filled square), anatase TiO_2 (diamond) and mixed anatase rutile phase (cross).

Considering lactic acid adsorption, the pollutant degradation rate in the presence of H_2O_2 tends to decrease with increasing adsorption; however, this decrease seems to depend on the TiO_2 phase type (Figure 4). This behavior can be explained by an enhancement in the formation of H_2O_2 complexes on the surface of TiO_2 leading to a greater formation of reactive oxygen species (ROS). These results agree with the impact that H_2O_2 degradation has on LA degradation (Figure 5).

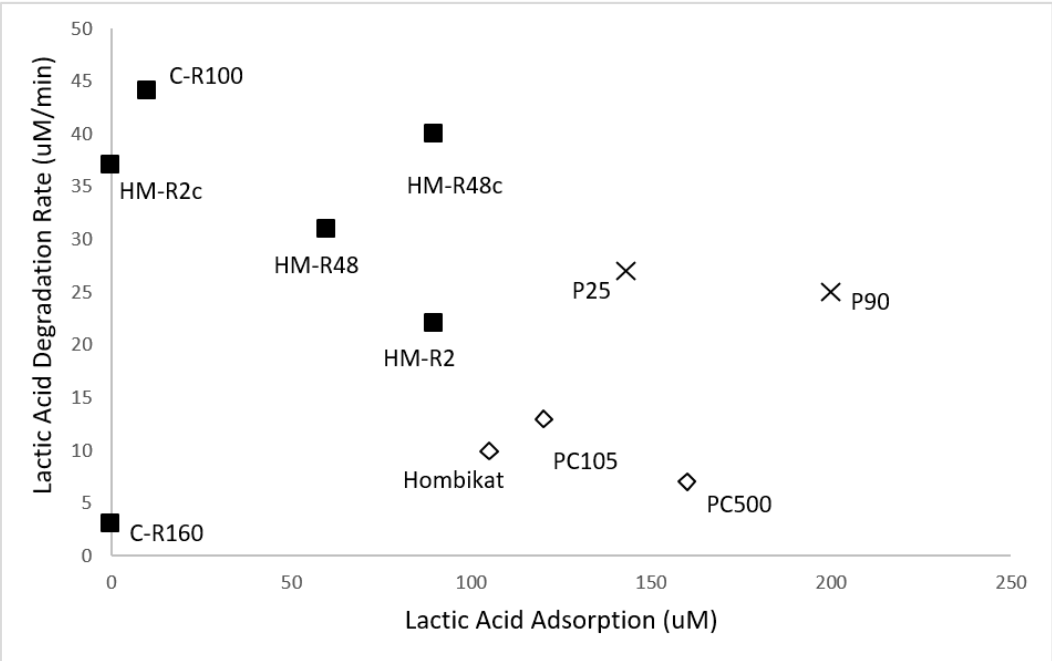

Figure 4. LA degradation rate in the presence of rutile TiO_2 (filled squares), anatase TiO_2 (diamonds), and mixed anatase/rutile TiO_2 (cross) as a function of LA adsorption.

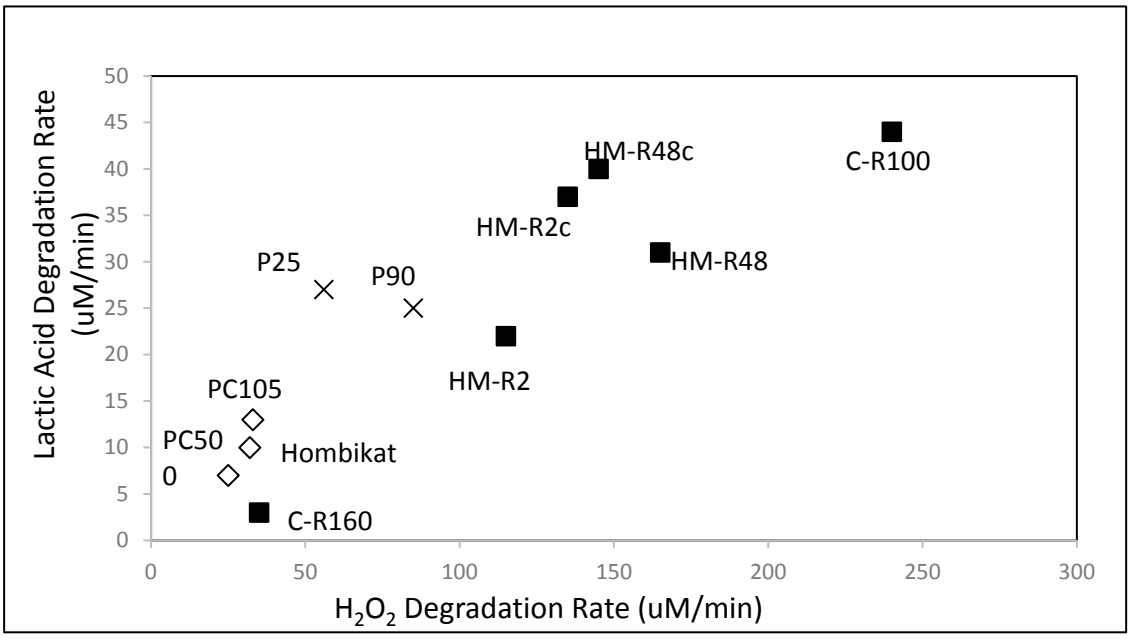

Figure 5. Lactic acid degradation rate as a function of H_2O_2 degradation rate for various TiO_2 samples.

Regardless of which TiO_2 phase is used, the degradation of LA in the presence of H_2O_2 is directly correlated to the decomposition of H_2O_2 as observed in Figure 5. This clearly indicates that the degradation of lactic acid is due to the activation of the complex formed between TiO_2 and H_2O_2.

While our results clearly show that LA degradation is correlated to the decomposition of an H_2O_2 complex formed on the surface of TiO_2, the negative impact of the surface area on the LA degradation rate is difficult to understand. Indeed, in the absence of H_2O_2, increasing the surface area of TiO_2 improves pollutant degradation [22,26]. In combination with our results showing the decomposition of H_2O_2 increasing as a function of the surface area, LA degradation should also increase with surface area. However, this is not the case. Moreover, we observe that depending on the nature of the TiO_2 phase, the impact of the surface area differs. A more negative impact was found for rutile TiO_2, whereas the surface area has much less of an impact on anatase TiO_2.

This behavior could be explained by an increase in the deactivation of reactive oxygen species on the surface of TiO_2 with increasing surface area. The varying degree of deactivation on anatase and rutile phases is potentially due to the different active species generated due to the more important amount of H_2O_2 adsorbed on important surface area. Active species initially formed could react with the more important amount of H_2O_2 adsorbed on more important surface area.

On rutile TiO_2, OH° generated by the decomposition of peroxo-complexes can react with H_2O_2 forming HO_2°, a less active species in comparison to OH° (Equation (5)):

$$OH^\circ + H_2O_2 \rightarrow HO_2^\circ + H_2O \quad (5)$$

While HO_2°, which is generated in the anatase phase, can react with H_2O_2 to form OH°, this limits the negative impact of the surface area (Equation (6)):

$$HO_2^\circ + H_2O_2 \rightarrow OH^\circ + H_2O + O_2 \quad (6)$$

However, it is just a hypothesis which should be verified by determining the active species generated using a high surface area of TiO_2 compared to the small surface area of TiO_2.

2.3. Impact of H_2O_2 on the Chemical Pathways of Lactic Acid Photocatalytic Degradation

Two initial chemical pathways can occur during the degradation of lactic acid: either decarboxylation or dehydrogenation, giving ethanol and pyruvic acid, respectively. Unfortunately, ethanol cannot be detected due to the sensitivity of our analyses, but also due to its reactivity towards hydroxyl radicals. Ethanol behaves as a scavenger of hydroxyl radicals [27]. The pathways were evaluated based on the detection of acetic acid and pyruvic acid.

Regardless of which TiO_2 sample is used, the main product detected in the aqueous phase and in the presence of H_2O_2 is acetic acid (Figure 6b). In the absence of H_2O_2, acetic acid is not initially present for anatase and anatase-containing samples, but is observed in the majority of rutile samples (Figure 6a).

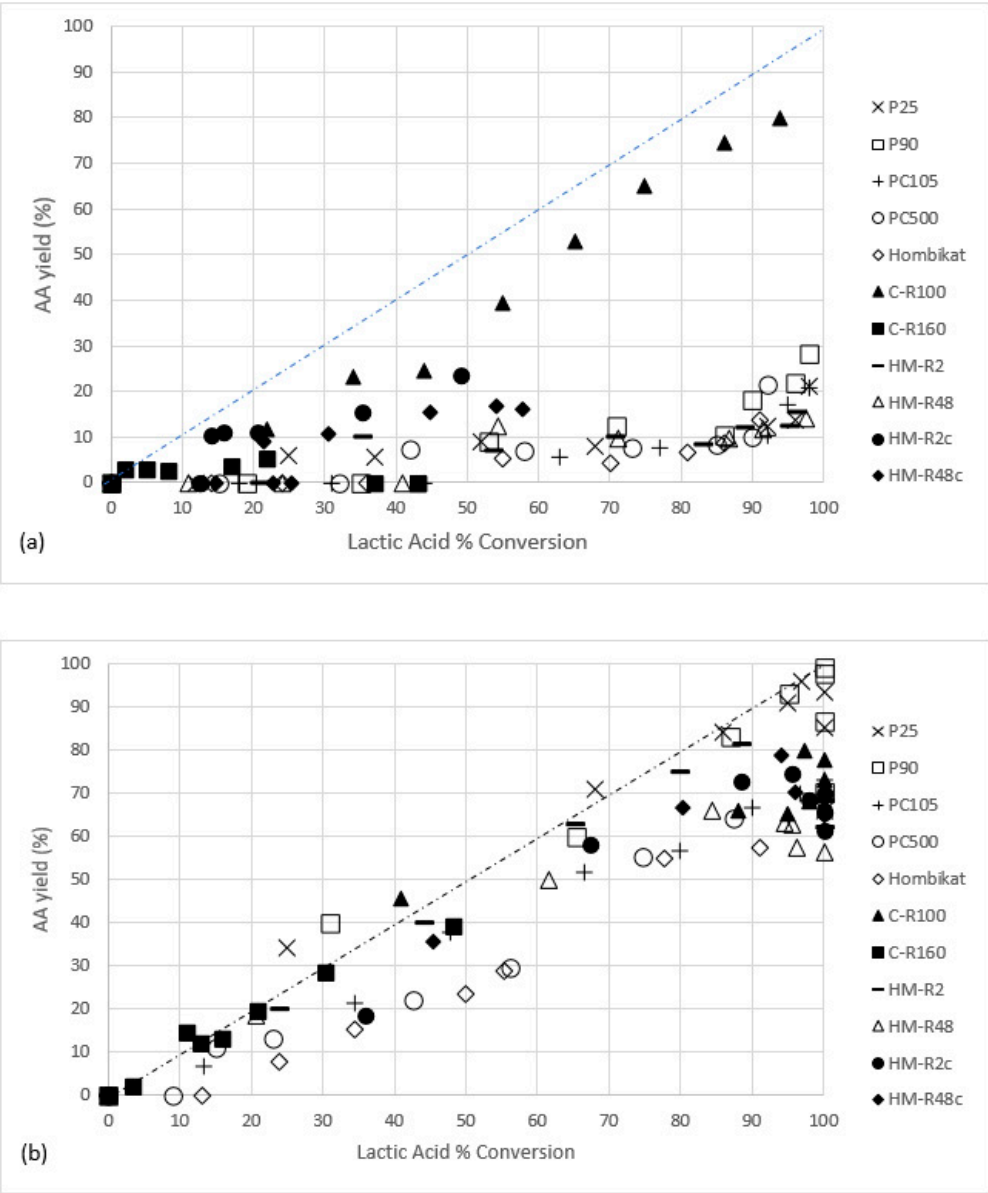

Figure 6. Acetic acid yield as a function of lactic acid conversion (**a**) without H_2O_2 and (**b**) with H_2O_2 in the presence of various catalysts. Dotted line corresponds to 100% of selectivity.

In the presence of H_2O_2, the acetic acid yield is lower for anatase than for samples containing rutile. These results agree with the formation of $HO_2°$, which is less active than OH°. It is also interesting to note that pyruvic acid formed from the initial dehydrogenation of OH groups appears

after about 60% LA conversion for all of the catalysts, except for the two commercial rutile samples where it is detected before 60% (Figure 7a). Its detection is attributed to the partial decomposition of H_2O_2, allowing for the direct adsorption of LA and immediate photocatalytic degradation. In fact, more than half of the H_2O_2 is degraded on a majority of the catalysts, and about 30% is degraded for P25 and P90 samples (Figure 7b).

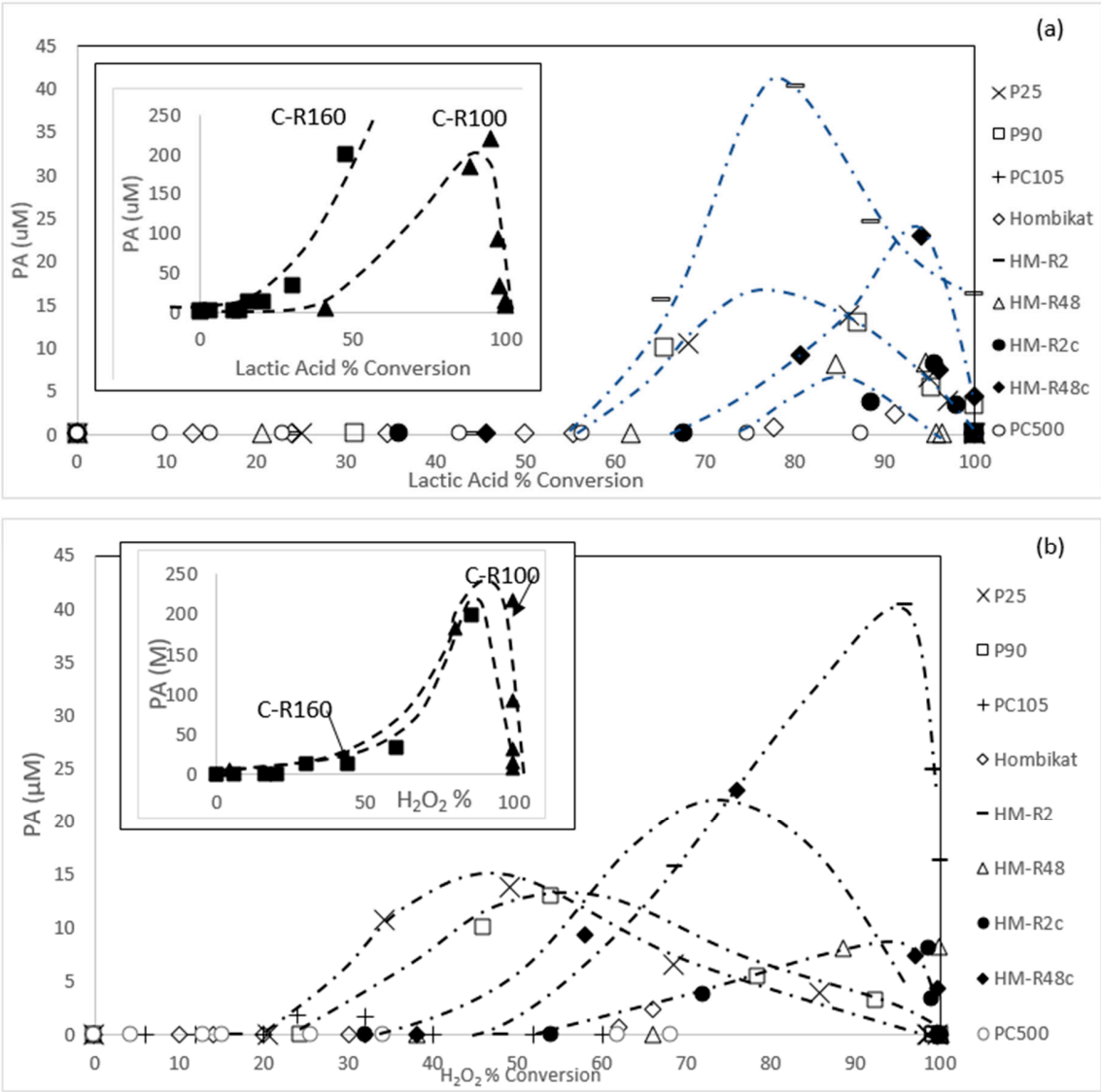

Figure 7. Pyruvic acid concentration as a function of lactic acid conversion (**a**) and of H_2O_2 conversion (**b**).

In the presence of H_2O_2, the absence of pyruvic acid at low LA conversion and the high formation of acetic acid supports the hypothesis that lactic acid undergoes rapid decarboxylation upon the generation of OH° radicals.

2.4. *Visible Photocatalytic Efficiency of TiO_2 Rutile and P25 in Presence of H_2O_2*

Previously, our results showed that the photocatalytic degradation of LA and formic acid (FA) upon irradiation and in the presence of H_2O_2 and TiO_2 is correlated to the decomposition of H_2O_2. As the H_2O_2 peroxo-complex also absorbs light in the visible region, we tested the degradation of FA and LA using a rutile TiO_2 sample and visible irradiation.

Prior to investigating the impact of H_2O_2 on the photocatalytic degradation of the pollutant under visible light, a control experiment was carried out in the absence of H_2O_2. It is clear that degradation is non-negligible in the presence of rutile TiO_2 (Figure 8). These results are consistent with the visible absorption of rutile TiO_2 (absorbance drops off past 413 nm).

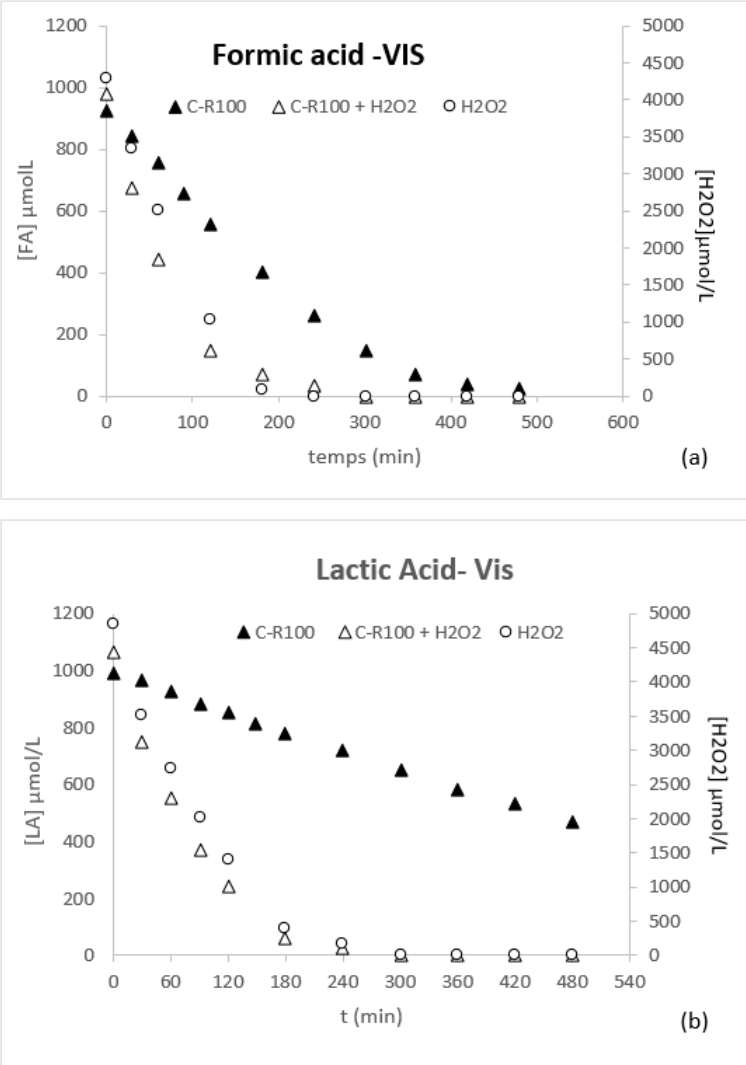

Figure 8. Degradation of FA and H_2O_2 (**a**) and LA and H_2O_2 (**b**) as a function of time in the presence of C-R100.

In the presence of H_2O_2, a significant enhancement in the degradation of FA and LA was observed, which was found to correlate directly with the decomposition of H_2O_2 (Figure 8a,b). Moreover, the disappearance rates of FA and LA are the same (6.7 µmol/L/min) with an H_2O_2 disappearance rate of about 28 µmol/L/min. In the case of FA, decarboxylation can occur, whereas with LA, both dehydrogenation and decarboxylation can occur [28]. To track their formation, we studied the intermediate products generated from LA under visible light irradiation. As shown in Figure 9a, in the presence of H_2O_2, only acetic acid was detected using visible light irradiation. This indicates that only decarboxylation occurs, which explains the comparable degradation rates for LA and FA.

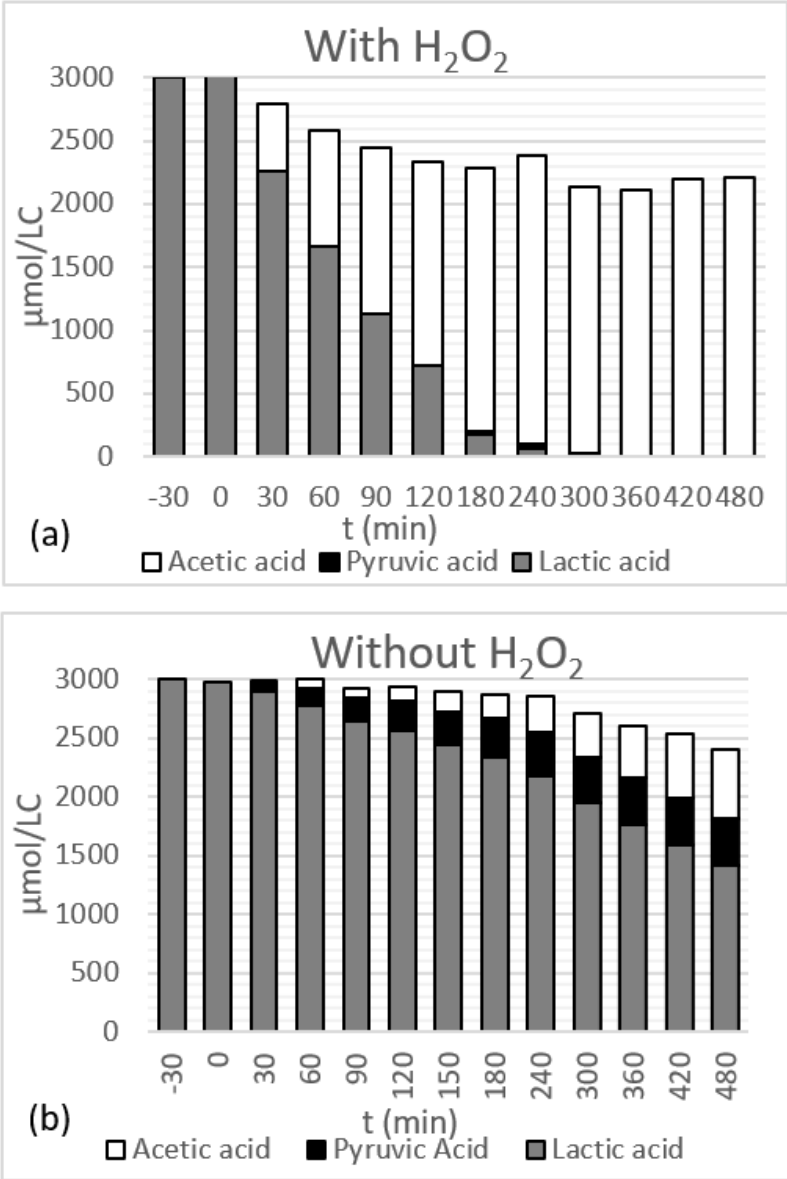

Figure 9. Carbon balance of the degradation of LA in the presence (**a**) and the absence (**b**) of H_2O_2, including the formation of acetic acid and pyruvic acid and the degradation of LA.

In the absence of H_2O_2 and under visible light exposure, the first step is likely to be dehydrogenation to form pyruvic acid (Figure 9b). A similar behavior has been observed in the presence of rutile under UV irradiation [28].

Comparing to the efficiency observed under UV sources, the photocatalytic efficiency under visible irradiation is lower, about seven times smaller than the photocatalytic efficiency observed under UV irradiation at 365 nm. This difference is due to lower absorption of the H_2O_2 complex formed on the surface of the catalyst above 400 nm compared to its absorption under UV but also to the number of photons emitted by these two irradiation sources, about $4.6 \cdot 10^{15}$ photons/s/cm^2 under visible light and 7.3 photons/s/cm^2 under UV light. Concerning the degradation mechanism under UV and visible light, in both cases, it is due to the decomposition of the H_2O_2 complex confirmed by the similar ratio of 4–5 observed between the degradation of organic pollutant and H_2O_2 decomposition and to the main formation of acetic acid under these two irradiation sources.

The efficiency of TiO_2 under visible light in the presence of H_2O_2 has already been mentioned by several authors studying different molecules (terebutylazine [15], Linuron [18], Prometryn [19],

salicylic acid [20] and decene [21]). Li et al. [20] propose a mechanism involving photoinduced electron transfer from the surface complexes of Ti(IV)–OOH. Ohno et al [21] considered the possibility of a photochemical reaction involving TiO_2^- peroxide. Tang et al. [15] suggests that in the presence of rutile TiO_2 the reaction occurs in the solution, while in the presence of anatase phase, heterogeneous reactions occur. Rao et al [18] also showed that the demethoxylation and demethylation of linuron are the main reactions, and dechlorination and hydroxylation are only minor reactions.

In our conditions, we showed that decarboxylation is the major reaction pathway, favored over dehydrogenation.

3. Materials and Methods

3.1. Chemicals

Formic acid (99%) and lactic acid (80%), for the photocatalytic degradation tests, were supplied, respectively, by Acros Organics (Geel, Belgium) and Sigma Aldrich Chemie S.A.R.L. (Saint-Quentin Fallavier, France). Pyruvic acid (100%) and acetic acid (99.7%), intermediate products formed in the degradation of lactic acid, were supplied by Sigma Aldrich Chemie S.A.R.L. H_2O_2 (50%) was purchased from Acros Organics. Ultrapure water (18 MΩ·cm^{-1}) was used throughout all of the experiments.

3.2. Catalysts

Eleven titanium dioxide samples were used: two commercial TiO_2 samples composed of 80% anatase and 20% rutile (TiO_2 P-25 and TiO_2 P-90) from Evonik, Essen, Nordrhein-Westfalen, two commercial anatase structures (PC105 and PC-500) from Millennium Chemicals (Hunt-Valley, MD, USA), and one (Hombikat UV100) purchased from Sachtleben Chemie GmbH (Duisburg, Germany), two commercial rutile structures (MPT-625 or C-R100, and C-R160) from Ishihara Sangyo Kaisha Ldt (Osaka, Japan) and Nanostructured, respectively, and four home-made TiO_2 rutile catalysts synthesized from $TiCl_4$ and hydrolyzed for either 2 h or 48 h. The non-calcined samples were named HM-R2 and HM-R48, and the calcined samples were named HM-R2c and HM-R48c. A detailed description of these photocatalysts was given in our previous work [28].

The characterizations of these catalysts are given in Table 1.

Table 1. Structure, surface area, Iso Electric Point (IEP) and crystallite size of each photocatalyst.

Photo-Catalysts	Structure	S_{BET} ($m^2 \cdot g^{-1}$)	Crystallite Size (nm)	IEP	Reference
P25	80% Anatase 20% Rutile	50	21–30	7 – 6.4	[29,30]
P90	80% Anatase 20% Rutile	90	14	7 – 6.6	[29,30]
PC 105	100% Anatase	88	15–25	4.7 +/− 0.5	[28]
PC 500	100% Anatase	340	5–10	6.2	[29]
UV 100	100% Anatase	300	<10	5.3	[30]
C-R100 (MPT 625)	100% Rutile	103	13	5.4 +/− 0.5	[28]
C-R160	100% Rutile	160	8–10	5.1 +/− 0.5	[28]
HM-R2	100% Rutile	173	7.5	4.3	[28]
HM-R2c	100% Rutile	112	9.9	3.5	[28]
HM-R48	100% Rutile	117	10.5	4.4	[28]
HM-R48c	100% Rutile	92	12.8	3.6	[28]

3.3. Photocatalytic Experiments and Analytical Procedures

The photocatalytic experiments were conducted using an aqueous solution of about 1000 μM lactic acid (LA) or formic acid (FA) and 5000 μM H_2O_2. The reactions were carried out in Pyrex photoreactors. For all degradation experiments, 1 g·L^{-1} of photocatalyst was used. A PLL18W Philips lamp and an HPK 125 W mercury lamp (Koninklijke Philips N.V., Amsterdam, The Netherlands) with

a filter cutting all wavelengths above 340 nm were used for the LA and FA experiments, respectively. In all cases, the UV irradiation was centered at 365 nm. A white LED emitting from 400 to 880 nm was used for visible irradiation. Prior to UV irradiation, the catalyst suspensions were allowed to reach adsorption equilibrium by stirring in the dark for 1 h. Samples of the reaction solution were taken periodically for several hours during UV or visible irradiation, filtered on a DURAPORE 0.45 µm hydrophilic membrane (Merck Millipore, Burlington, MA, USA) to remove the photocatalyst, and used for further analysis.

3.4. Analytical Procedure

H_2O_2 was complexed with an acidic solution of $TiCl_4$. Then, the H_2O_2 content of each sample was monitored at 410 nm by performing UV–vis spectroscopy in order to detect the yellow complex which forms under acidic conditions in the presence of Ti^{4+} ions [31,32].

The samples were analyzed with a Shimadzu (Shimadzu Corporation, Kyoto, Japan) High Performance Liquid Chromatograph (HPLC) equipped with a Coregel-87H3 column (300 mm × 7.8 mm—Concise Separations) thermo-stated at 30 °C. A H_2SO_4 (5×10^{-3} mol·L^{-1}) mobile phase was used at a flow rate of 0.7 mL·min^{-1}. A diode array detector was used and set at 210 nm.

4. Conclusions

When studying the impact of H_2O_2, we found that utilizing it in combination with rutile TiO_2 greatly favors the oxidation of FA and LA. No additional improvement was observed in the presence of anatase TiO_2 under the same conditions. The higher the amount of rutile in the TiO_2 photocatalyst, the more significant the improvement.

By using 11 commercial and home-made TiO_2 samples to study the degradation of LA, we also showed that the improvement depends on the surface area of TiO_2. Opposing our results observed in the absence of H_2O_2, an increase in the surface area is harmful to the degradation. However, regardless of which TiO_2 sample is used, the degradation of LA is always correlated to the decomposition of H_2O_2.

The larger the surface area, the less lactic acid is degraded in the presence of H_2O_2. While the impact is significant in the rutile phase, in the presence of pure anatase or anatase mixed with 20% rutile TiO_2, an increase in surface area has much less of an impact. This behavior could be explained by an increase in the deactivation of ROS on the surface of TiO_2 with increasing surface area. The varying degrees of deactivation on anatase and rutile phases are potentially due to the different active species generated. On rutile TiO_2, OH° is generated by the decomposition of peroxo-complexes. It can then react with H_2O_2 forming HO_2°, a less active species in comparison to OH°. While HO_2°, which is generated in the anatase phase, can react with H_2O_2 to form OH°, this limits the negative impact of the surface area.

Our work also highlights a modification in the chemical pathways of LA in the presence of H_2O_2. Regardless of which TiO_2 sample is used, the formation of acetic acid was favored suggesting a promotion of the decarboxylation reaction over the dehydrogenation reaction.

Our investigation into the performance of H_2O_2 on rutile TiO_2 exposed to visible irradiation indicates that, for both UV and visible light, the mechanism of H_2O_2/TiO_2 light-driven photocatalysis is ascribed to the chemisorption of H_2O_2 on the surface of TiO_2 and the subsequent formation of a yellow surface complex, which is decomposed into ROSs. This mechanism is confirmed by the existence of a strong correlation between the decomposition of H_2O_2 and degradation of LA/FA under visible and UV irradiation. Moreover, we highlight that the photocatalytic degradation rates of FA and LA under visible light are identical, indicating that the decarboxylation reaction is the main pathway in the degradation of LA under visible light. This is also in agreement with our observation of acetic acid formation alone, whereas in the absence of H_2O_2, the first step is likely dehydrogenation.

These studies show that visible light, and consequently, solar light, can be efficiently used for removing some organic pollutants by photocatalysis in the presence of H_2O_2, and also by utilizing

rutile TiO_2. It could potentially also be applicable for valorization reactions. In the future, it will be insightful to investigate the degradation of different families of molecules and their chemical pathways under visible and/or UV irradiation.

Author Contributions: A.H. and M.H. performed the lactic acid experiments and participate to the redaction of the publication. K.S. and F.D. performed the formic acid experiments. F.D. developed the analyses of H_2O_2, lactic acid, pyruvic acid and acetic acid. C.G. designed the experiments and complemented the writing and interpretations made by A.H. All authors have read and agreed to the published version of the manuscript.

Funding: This project was funded in part by the National Science Foundation (Award #1560390) for scholarship of A.H., the financial support of the Algerian Ministry of Education and Research for K.S. and CNRS at the University of Lyon 1 for the running cost.

Acknowledgments: The authors gratefully acknowledge National Science Foundation, the financial support of the Algerian Ministry of Education, CNRS and University Lyon 1.

Conflicts of Interest: The authors declare no conflict of interest.

References

1. Ohno, T.; Mitsui, T.; Matsumura, M. TiO_2-photocatalyzed oxidation of adamantane in solutions containing oxygen or hydrogen peroxide. *J. Photochem. Photobiol. A Chem.* **2003**, *160*, 3–9. [CrossRef]
2. Amalric, L.; Guillard, C.; Pichat, P. Use of catalase and superoxide dismutase to assess the roles of hydrogen peroxide and superoxide in the TiO_2 or ZnO photocatalytic destruction of 1,2-dimethoxybenzene in water. *Res. Chem. Intermed.* **1994**, *20*, 579–594. [CrossRef]
3. Barakat, M.A.; Tseng, J.M.; Huang, C.P. Hydrogen peroxide-assisted photocatalytic oxidation of phenolic compounds. *Appl. Catal. B Environ.* **2005**, *59*, 99–104. [CrossRef]
4. Chemseddine, A.; Boehm, H.P. A study of the primary step in the photochemical degradation of acetic acid and chloroacetic acids on a TiO_2 photocatalyst. *J. Mol. Catal.* **1990**, *60*, 295–311. [CrossRef]
5. Doong, R.; Chang, W. Photoassisted titanium dioxide mediated degradation of organophosphorus pesticides by hydrogen peroxide. *J. Photochem. Photobiol. A Chem.* **1997**, *107*, 239–244. [CrossRef]
6. Harada, K.; Hisanaga, T.; Tanaka, K. Photocatalytic degradation of organophosphorous insecticides in aqueous semiconductor suspensions. *Water Res.* **1990**, *24*, 1415–1417. [CrossRef]
7. Silva, A.M.T.; Nouli, E.; Xekoukoulotakis, N.P.; Mantzavinos, D. Effect of key operating parameters on phenols degradation during H_2O_2-assisted TiO_2 photocatalytic treatment of simulated and actual olive mill wastewaters. *Appl. Catal. B Environ.* **2007**, *73*, 11–22. [CrossRef]
8. Tanaka, K.; Hisanaga, T.; Harada, K. Efficient photocatalytic degradation of chloral hydrate in aqueous semiconductor suspension. *J. Photochem. Photobiol. A Chem.* **1989**, *48*, 155–159. [CrossRef]
9. Vorontsov, A.V.; Savinov, E.V.; Davydov, L.; Smirniotis, P.G. Photocatalytic destruction of gaseous diethyl sulfide over TiO_2. *Appl. Catal. B Environ.* **2001**, *32*, 11–24. [CrossRef]
10. Monteagudo, J.M.; Durán, A.; San Martín, I.; Vellón, B. Photocatalytic degradation of aniline by solar/TiO_2 system in the presence of the electron acceptors $Na_2S_2O_8$ and H_2O_2. *Sep. Purif. Technol.* **2020**, *238*, 116456. [CrossRef]
11. Fan, G.; Zhan, J.; Luo, J.; Zhang, J.; Chen, Z.; You, Y. Photocatalytic degradation of naproxen by a H_2O_2-modified titanate nanomaterial under visible light irradiation. *Catal. Sci. Technol.* **2019**, *9*, 4614–4628. [CrossRef]
12. Feilizadeh, M.; Attar, F.; Mahinpey, N. Hydrogen peroxide-assisted photocatalysis under solar light irradiation: Interpretation of interaction effects between an active photocatalyst and H_2O_2. *Can. J. Chem. Eng.* **2019**, *97*, 2009–2014. [CrossRef]
13. Cuerda-Correa, E.M.; Alexandre-Franco, M.F.; Fernández-Gonzále, C. Advanced Oxidation Processes for the Removal of Antibiotics from Water. An Overview. *Water* **2020**, *12*, 102. [CrossRef]
14. Sujatha, G.; Shanthakumar, S.; Chiampo, F. UV Light-Irradiated Photocatalytic Degradation of Coffee Processing Wastewater Using TiO_2 as a Catalyst. *Environments* **2020**, *7*, 47. [CrossRef]
15. Tang, J.; Chen, Y.; Dong, Z. Effect of crystalline structure on terbuthylazine degradation by H_2O_2-assisted TiO_2 photocatalysis under visible irradiation. *J. Environ. Sci.* **2019**, *79*, 153–160. [CrossRef]
16. Hirakawa, T.; Yawata, K.; Nosaka, Y. Photocatalytic reactivity for $O_2\bullet^-$ and OH• radical formation in anatase and rutile TiO_2 suspension as the effect of H_2O_2 addition. *Appl. Catal. Gen.* **2007**, *325*, 105–111. [CrossRef]

17. Zhang, J.; Nosaka, Y. Mechanism of the OH Radical Generation in Photocatalysis with TiO_2 of Different Crystalline Types. *J. Phys. Chem. C* **2014**, *118*, 10824–10832. [CrossRef]
18. Rao, Y.F.; Chu, W. Reaction Mechanism of Linuron Degradation in TiO_2 Suspension under Visible Light Irradiation with the Assistance of H_2O_2. *Environ. Sci. Technol.* **2009**, *43*, 6183–6189. [CrossRef]
19. Li, Q.K.; Zhou, B.Y.; Tang, J.; Chen, Y.Q. Degradation of prometryn by TiO_2 visible photocatalysis with H_2O_2 assistance. *J. Zhengzhou Univ. (Eng. Sci.)* **2014**, *35*, 55–59.
20. Li, X.Z.; Chen, C.C.; Zhao, J.C. Mechanism of Photodecomposition of H_2O_2 on TiO_2 Surfaces under Visible Light Irradiation. *Langmuir* **2001**, *17*, 4118–4122. [CrossRef]
21. Ohno, T.; Masaki, Y.; Hirayama, S.; Matsumura, M. TiO_2-Photocatalyzed Epoxidation of 1-Decene by H_2O_2 under Visible Light. *J. Catal.* **2001**, *204*, 163–168. [CrossRef]
22. Lousada, C.M.; Johansson, A.J.; Brinck, T.; Jonsson, M. Mechanism of H_2O_2 Decomposition on Transition Metal Oxide Surfaces. *J. Phys. Chem. C* **2012**, *116*, 9533–9543. [CrossRef]
23. Einsenberg, G. Colorimetric Determination of Hydrogen Peroxide. *Ind. Eng. Chem. Anal. Ed.* **1943**, *15*, 327–328. [CrossRef]
24. Rodier, J.; Legube, B.; Merlet, N.; Brunet, R. *L'analyse de L'eau*, 9th ed.; Dunod: Paris, France, 2009.
25. Huang, W.F.; Raghunath, P.; Lin, M.C. Computational study on the reactions of H_2O_2 on TiO_2 anatase (101) and rutile (110) surfaces. *J. Comp. Chem.* **2010**, *32*, 1065–1081. [CrossRef] [PubMed]
26. Sahel, K.; Elsellami, L.; Mirali, I.; Dappozze, F.; Bouhent, M.; Guillard, C. Hydrogen peroxide and photocatalysis. *Appl. Catal. B Environ.* **2016**, *188*, 106–112. [CrossRef]
27. Buchalska, M.; Kobielusz, M.; Matuszek, A.; Pacia, M.; Wojtyła, S.; Macyk, W. On Oxygen Activation at Rutile- and Anatase-TiO_2. *ACS Catal.* **2015**, *5*, 7424–7431. [CrossRef]
28. Holm, A.; Hamandi, M.; Simonet, F.; Jouguet, B.; Dappozze, F.; Guillard, C. Impact of rutile and anatase phase on the photocatalytic decomposition of lactic acid. *Appl. Catal. B Environ.* **2019**, *253*, 96–104. [CrossRef]
29. Gumy, D.; Morais, C.; Bowen, P.; Pulgarin, C.; Giraldo, S.; Hajdu, R.; Kiwi, J. Catalytic activity of commercial of TiO_2 powders for the abatement of the bacteria (*E. coli*) under solar simulated light: Influence of the isoelectric point. *Appl. Catal. B Environ.* **2006**, *63*, 76–84. [CrossRef]
30. Doudrick, K.; Monzon, O.; Mangonon, A.; Hristovski, K.; Westerhoff, P. Nitrate reduction in water using commercial titanium dioxide photocatalysts (P25, P90, and Hombikat UV100). *J. Environ. Eng.* **2012**, *138*, 852–861. [CrossRef]
31. Sánchez, L.D.; Taxt-Lamolle, S.F.M.; Hole, E.O.; Krivokapić, A.; Sagstuen, E.; Haugen, H.J. TiO_2 suspension exposed to H_2O_2 in ambient light or darkness: Degradation of methylene blue and EPR evidence for radical oxygen species. *Appl. Catal. B Environ.* **2013**, *142*, 662–667. [CrossRef]
32. Feierman, D.E.; Winston, G.W.; Cederbaum, A.I. Ethanol oxidation by hydroxyl radicals: Role of iron chelates, superoxide, and hydrogen peroxide. *Alcohol Clin. Exp. Res.* **1985**, *9*, 95–102. [CrossRef] [PubMed]